Widespread Genetic Incompatibility in *C. Elegans* Maintained by Balancing Selection

Hannah S. Seidel,*† Matthew V. Rockman,*† Leonid Kruglyak*

Natural selection is expected to eliminate genetic incompatibilities from interbreeding populations. We have discovered a globally distributed incompatibility in the primarily selfing species *Caenorhabditis elegans* that has been maintained despite its negative consequences for fitness. Embryos homozygous for a naturally occurring deletion of the zygotically acting gene *zeel-1* arrest if their sperm parent carries an incompatible allele of a second, paternal-effect locus, *peel-1*. The two interacting loci are tightly linked, with incompatible alleles occurring in linkage disequilibrium in two common haplotypes. These haplotypes exhibit elevated sequence divergence, and population genetic analyses of this region indicate that natural selection is preserving both haplotypes in the population. Our data suggest that long-term maintenance of a balanced polymorphism has permitted the incompatibility to persist despite gene flow across the rest of the genome.

*C*aenorhabditis elegans is a globally distributed species of free-living bacteria-eating nematode. Although rare males contribute at a low rate to outcrossing, *C. elegans* occurs primarily as inbred self-fertilizing hermaphrodites (*1–4*). A wild isolate from Hawaii, CB4856, has been identified among well-studied isolates as the most divergent at the sequence level from the standard laboratory strain, N2, derived from an isolate from Bristol, England (*5–7*). As a result of this sequence divergence, the Hawaiian strain is widely used to map mutations induced in the Bristol background.

Genetic incompatibility between Bristol and Hawaii. We generated recombinant inbred lines (RILs) from the 10th generation of an advanced intercross between Bristol and Hawaii to

Lewis-Sigler Institute for Integrative Genomics and Department of Ecology and Evolutionary Biology, Princeton University, Princeton, NJ 08544, USA.

*To whom correspondence should be addressed. E-mail: hseidel@princeton.edu (H.S.S.); mrockman@princeton.edu (M.V.R.); leonid@genomics.princeton.edu (L.K.)
†These authors contributed equally to this work.

study natural genetic variation in *C. elegans*, and we genotyped the RILs at 1450 single-nucleotide polymorphism (SNP) markers (*8*). We noted that a region on the left arm of chromsome I exhibited a dramatic deficit of Hawaii alleles among the RILs. Of 239 RILs, only 5 carried the Hawaii allele at the most skewed marker, and simulations of the intercross pedigree indicated that this allele frequency skew could not have arisen by drift, suggesting that selection had acted during construction of the RILs (fig. S1). We then crossed Hawaii to a Bristol strain carrying a visible marker located 10 cM from the most skewed RIL marker, and we examined F_2 progeny produced by self-fertilizing F_1 hermaphrodites. Surprisingly, approximately 25% of F_2 progeny arrested as embryos, and embryonic lethality segregated opposite the visible marker (Table 1). F_2 lethality was not an effect of the marker: Self-fertilizing F_1 hermaphrodites derived from reciprocal crosses between Hawaii and wild-type Bristol produced 25% dead embryos, as did F_1 hermaphrodites mated to F_1 males (Fig. 1).

Lethality caused by a paternal effect by zygotic interaction. The segregation of embryonic lethality opposite the visible marker implied that the arrested embryos represented those homozygous for the Hawaii allele of a locus linked to the marker, on the left arm of chromosome I. Because embryonic lethality within the Hawaii strain itself is very low (less than 1%), we reasoned that F_2 lethality reflected an incompatibility between the Hawaii allele of this locus and an element in the Bristol genome. We also reasoned that it did not reflect two synthetically lethal alleles segregating in the F_2 population because such an interaction would affect less than one-quarter of F_2 embryos (up to 3/16, depending on linkage and dominance). One-quarter lethality is expected, however, if the incompatibility involves an interaction between the genotype of the zygote and a maternal or paternal effect.

To test this possibility, Hawaii × Bristol F_1 males and hermaphrodites were separately back-crossed to Hawaii individuals, and lethality was scored among the resulting embryos. We observed 50% lethality when F_1 males were mated to Hawaii hermaphrodites but less than 2% lethality in the reciprocal cross (Fig. 1). Thus, lethality depends on both paternal and zygotic genotype, but is independent of maternal cytoplasm. (Both Hawaii and F_1 hermaphrodites produced dead embryos, 50% and 25%, respectively, when mated to F_1 males.) In sum, lethality appears to result from a paternal effect by zygotic interaction, whereby embryos homozygous for the Hawaii allele of a zygotically acting locus fail to hatch when the sperm parent—male or hermaphrodite—is a Hawaii × Bristol heterozygote. An interaction between a paternal effect and a zygotically acting gene is surprising because sperm-supplied factors are expected to act during fertilization and first cleavage (*9*), whereas early embryogenesis is primarily controlled by maternally contributed factors, and zygotic transcription is not known to occur before the four-cell stage (*10*).

Tight linkage of the zygotically acting and paternal-effect loci. To understand the genetic basis of the incompatibility, we used the RILs

Table 1. F_2 lethality segregates opposite visible marker *bli-3*, located 10 cM from the most skewed RIL marker. Genotypes of F_2 progeny from selfing Bristol/*bli-3* and Hawaii/*bli-3* hermaphrodites were scored. Embryonic lethality from selfing Hawaii/*bli-3* hermaphrodites was slightly greater than 25% because the visible marker introduces a small percentage of lethality.

F_2 genotype	Bristol/*bli-3* hermaphrodite	Hawaii/*bli-3* hermaphrodite
bli-3/*bli-3*	21.7% (128)	21.8% (128)
bli-3/+	49.9% (295)	42.0% (246)
+/+	24.5% (145)	5.1% (30)
Arrested embryos	3.9% (23)	31.1% (182)

Fig. 1. Paternal effect by zygotic lethality. The percent of embryonic lethality (total) was scored from the crosses shown. Orange and blue indicate Bristol and Hawaii haplotypes, respectively. Pie charts show the proportions of embryos that hatched (white) and failed to hatch (black). F_1 individuals were derived from reciprocal Bristol × Hawaii crosses. Embryonic lethality from selfing Bristol and Hawaii hermaphrodites, reciprocal Bristol × Hawaii, and reciprocal Bristol × F_1 crosses was less than 0.8% (*n* > 240 embryos for each).

24.0%(880)   26.5%(1764)   50.4%(4432)   1.7%(4160)
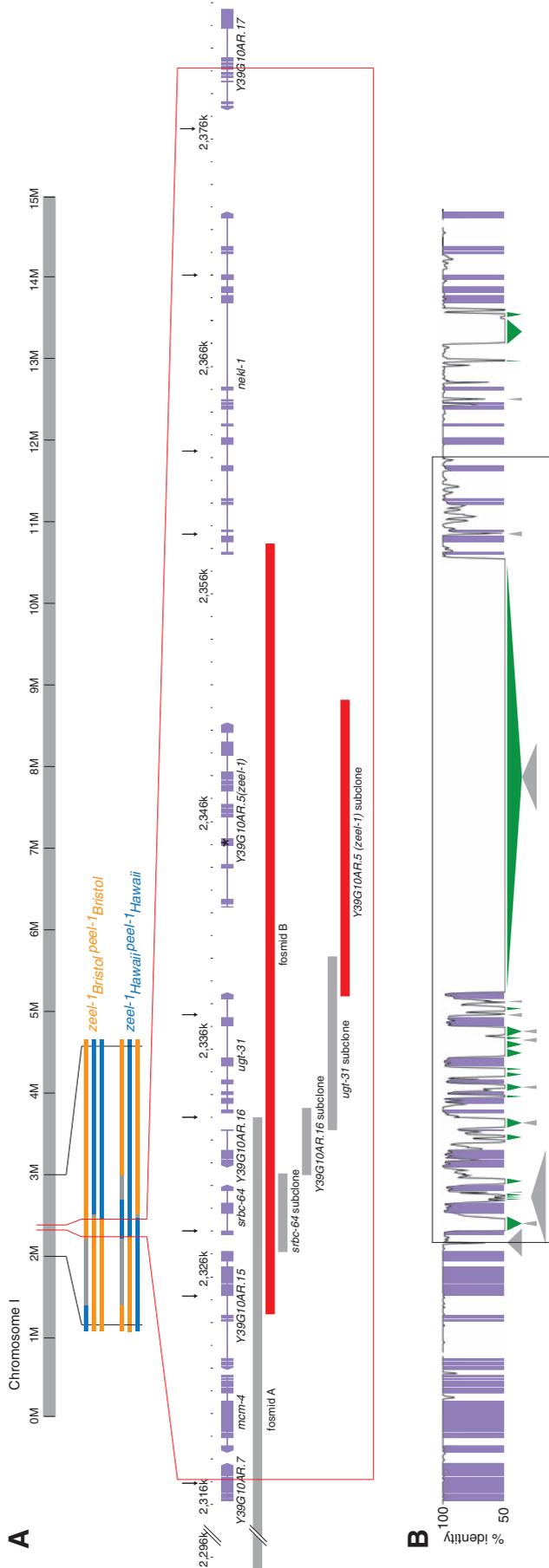
Fig. 2. *zeel-1* and *peel-1* map to the same 62-kb interval. (**A**) Colored bars represent Bristol (orange) and Hawaii (blue) haplotypes carried by six RILs used to map *zeel-1* and *peel-1*. Gray bars show regions between undetermined RIL breakpoints. RIL genotypes inferred from mapping crosses are shown to the right of the haplotypes. The red box in the middle indicates the interval to which *zeel-1* and *peel-1* map. Gene annotations derive from WormBase (ws170) gene models for Bristol. Horizontal bars indicate coverage of fosmid A (WRM0614dC06), fosmid B (WRM0633bE09), and subclones used in transgenic complementation, with rescuing transgenes in red. A black asterisk indicates the frame shift introduced into the *Y39G10AR.5* subclone. Arrows indicate markers used to genotype wild isolates. All markers are in complete linkage disequilibrium. (**B**) mVista alignment of Hawaii and Bristol sequence across a portion of the *zeel-1/peel-1* interval (34). We used default parameters and Bristol as the reference sequence. The black box surrounds the interval of elevated divergence between Bristol and Hawaii. Large (>50 bp) deletions (green) and insertions (gray) in Hawaii relative to the Bristol sequence are shown below the alignment.

to map both the zygotically acting locus, *zeel-1* (*zygotic epistatic embryonic lethal–1*), and the paternal-effect locus, *peel-1* (*paternal effect epistatic embryonic lethal–1*). We crossed RILs to Bristol and Hawaii and scored lethality among embryos laid by self-fertilizing F_1 hermaphrodites and Hawaii hermaphrodites mated to F_1 males. The pattern of lethality among F_2 and backcross embryos was consistent with each RIL carrying either the Bristol alleles of both *zeel-1* and *peel-1* or the Hawaii alleles of both. We identified only one genomic interval in which all lines of the former class carried the Bristol haplotype and all lines of the latter class carried the Hawaii haplotype. Thus, both *zeel-1* and *peel-1* map to this interval, a 62-kb region on chromosome I (position 2,317,234 to 2,379,249) (Fig. 2A). We confirmed tight linkage between the two loci; they do not segregate independently among backcross progeny (table S1).

Incomplete penetrance of the incompatibility. The penetrance of the incompatibility (i.e., the extent of lethality among *zeel-1*$_{Hawaii}$ homozygotes sired by *peel-1* heterozygotes) was complete when oocytes were fertilized by male sperm but incomplete when they were fertilized by hermaphrodite sperm. We collected embryos from self-fertilizing F_1 hermaphrodites and from F_1 hermaphrodites mated to F_1 males and genotyped surviving progeny at the *zeel-1* locus. Among self-progeny, approximately 10% of *zeel-1*$_{Hawaii}$ homozygotes survived to hatching, although most had retarded development and abnormal morphologies (8). In contrast, none survived when fertilized by F_1 males. Penetrance of the incompatibility also appeared complete among embryos from F_1 males backcrossed to Hawaii hermaphrodites, as these broods lacked the deformed larvae characteristic of surviving *zeel-1*$_{Hawaii}$ homozygotes.

The morphological defects of surviving *zeel-1*$_{Hawaii}$ homozygotes were highly variable and often similar to the terminal phenotype observed in arrested embryos, which usually showed tissue differentiation but no elongation past the twofold stage. Nevertheless, some *zeel-1*$_{Hawaii}$ homozygotes matured to adulthood and produced progeny. These progeny were entirely wild type, implying that the paternal effect is not caused by heritable defects such as DNA damage or aneuploidy in *zeel-1*$_{Hawaii}$ sperm.

Globally distributed incompatibility. To determine the distribution of alleles causing the Bristol-Hawaii incompatibility in the global *C. elegans* population, we phenotyped 62 wild isolates from 40 localities. From each locality, we phenotyped only strains known to be genetically distinct. We crossed each strain to Bristol and Hawaii and scored lethality among embryos from self-fertilizing F_1 hermaphrodites, F_1 males backcrossed to Hawaii hermaphrodites, and F_1 males backcrossed to hermaphrodites of the wild isolate itself. All but one wild isolate produced a pattern of lethality consistent with carrying either the Bristol alleles of both

peel-1 and zeel-1 (Bristol-compatible strains) or the Hawaii alleles of both (Hawaii-compatible strains). The exception, a strain collected from Roxel, Germany, was compatible with both Bristol and Hawaii, showing no lethality in crosses to either strain. The global distribution of Bristol-compatible and Hawaii-compatible strains demonstrates that the two classes are not geographically isolated (Fig. 3), which is consistent with an absence of large-scale population structure in C. elegans (1, 5, 11–13). Both classes were found in many localities, and individual samples of compost from two localities in northern Germany contained both Bristol- and Hawaii-compatible strains, indicating that the two classes co-occur at the most local level (11).

Molecular signatures of balancing selection. The interval to which zeel-1 and peel-1 map contains a region of dramatically elevated sequence divergence between the Bristol and Hawaii haplotypes. This region spans 33 kb of Bristol sequence and includes four full genes and part of a fifth (Fig. 2B). The Hawaii haplotype contains a 19-kb deletion spanning the gene Y39G10AR.5. Divergence within coding segments of the remaining genes averages 5%, which is 50 times higher than previous genome-wide estimates of pairwise divergence from both coding and noncoding sequence (6, 7). Noncoding segments in this region are largely unalignable and contain many insertions and deletions, mainly composed of repetitive elements. The left boundary of the divergent interval is abrupt and is marked by a 1-kb insertion in Hawaii. Genomic divergence within the 13 kb immediately outside the insertion is 0.1%. The right boundary is less abrupt, with divergence falling gradually to 0.7% across 4 kb.

We genotyped the wild isolates with markers located throughout the interval and found that all Hawaii-compatible strains carry Hawaii-like haplotypes, whereas all Bristol-compatible strains carry Bristol-like haplotypes (table S2). The doubly compatible strain carries a Bristol-like haplotype. Linkage disequilibrium among markers within the divergent interval is complete but breaks down for markers 165 kb to the left and 78 kb to the right of the interval.

To understand the cause of elevated polymorphism in the zeel-1/peel-1 interval, we sequenced the exons and adjacent regions of srbc-64, a gene located within the divergent interval, from 45 genetically distinct wild isolates. Elevated polymorphism may result from an elevated mutation rate, an ancient coalescence of neutral alleles, or long-term balancing selection maintaining divergent haplotypes against loss by genetic drift, thereby permitting them to accumulate more mutations than expected under neutrality (14). Under balancing selection, most mutations will differentiate the two major haplotype classes, creating an excess of intermediate-frequency alleles. Among the srbc-64 sequences, we observed 80 polymorphic sites but only six distinct haplotypes, far fewer than expected for a

neutral sample (P < 0.0001). Furthermore, the allele frequency spectrum was strongly skewed toward intermediate-frequency alleles (Tajima's D = 3.56, P < 0.0001). These data are consistent with long-term maintenance by balancing selection.

The srbc-64 sequences form two distinct, deeply branching clades, reflecting the Bristol-
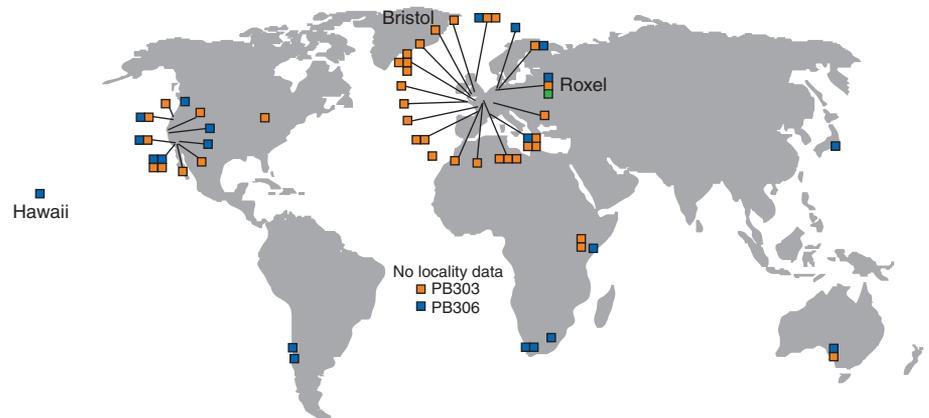
Fig. 3. Strains compatible with Bristol and incompatible with Hawaii (orange) and strains compatible with Hawaii and incompatible with Bristol (blue) are globally distributed. Strains compatible with both Bristol and Hawaii (green) derive from a locality in Roxel, Germany. For each locality, only strains known to be genetically distinct are shown. Strain names and localities are presented in table S7.
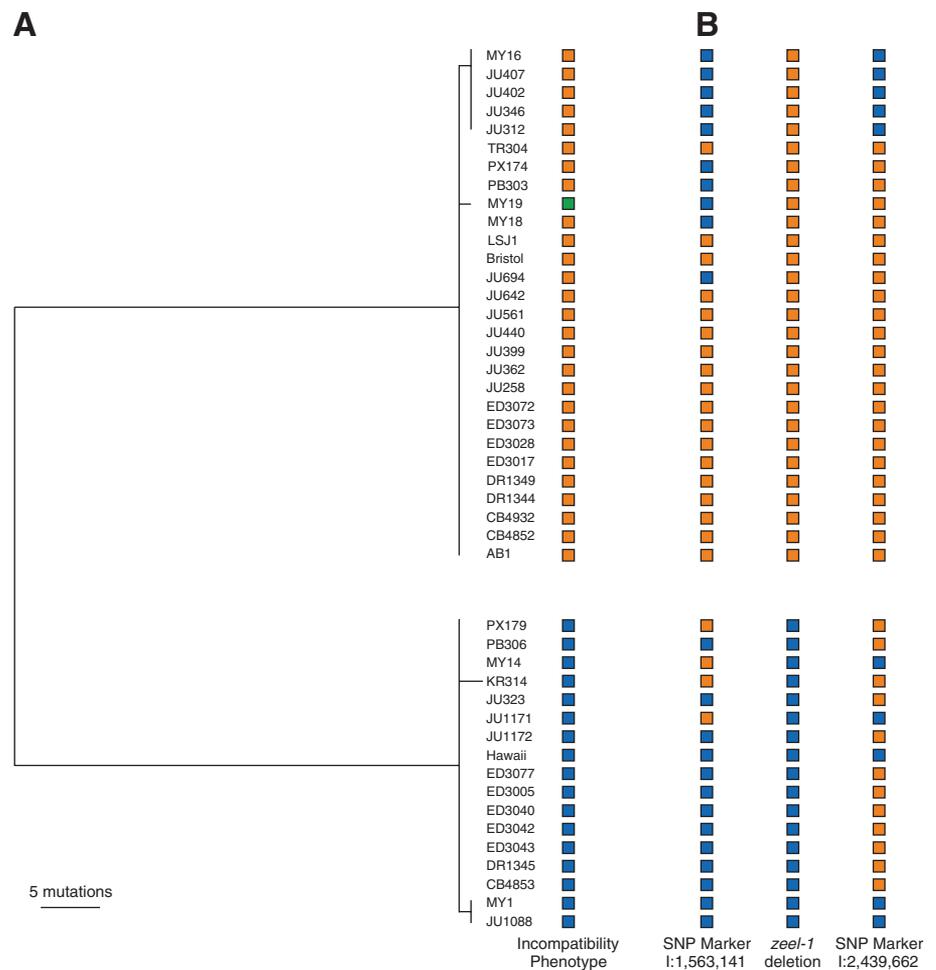
Fig. 4. Signature of balancing selection on the zeel-1/peel-1 interval. (**A**) Haplotypes of 1193 bp of the srbc-64 gene, excluding gapped sites, are split into two deeply divergent clades, one compatible with Bristol (orange) and one with Hawaii (blue). Doubly compatible MY19 (green) has a haplotype similar to that of Bristol. (**B**) Recombination has separated the zeel-1 deletion polymorphism from marker SNPs on both sides of the divergent interval.

and Hawaii-compatible classes (Fig. 4A). This topology is not representative of the genome as a whole. Markers on both sides of the divergent interval exhibit evidence of genetic exchange between the two classes (Fig. 4B), and phylogenies constructed from mitochondrial sequence and nuclear sequences located elsewhere in the genome do not resolve Bristol- and Hawaii-compatible strains into two distinct clades (5, 15), indicating that gene flow occurs across the rest of the genome.

The exceptional divergence between the Bristol and Hawaii haplotypes does not appear to be due to diversifying selection favoring amino acid–changing substitutions, nor to relaxed selection allowing degeneration of their protein-coding sequences. Despite synonymous divergence orders of magnitude above that observed for genes outside the interval, genes within the interval exhibit ratios of nonsynonymous to synonymous substitution of less than 0.2, consistent with purifying selection (Table 2). Given a direct estimate of the mutation rate ($\mu = 0.9 \times 10^{-8}$ per site per generation) (16), the estimated divergence at synonymous sites implies that the incompatible haplotypes diverged roughly 8 million generations ago.

Identification of zeel-1. We cloned *zeel-1* by introducing two fosmids carrying Bristol genomic DNA that together covered 45 kb of the 62-kb *zeel-1* interval into the Hawaii background (Fig. 2A). To test for rescue, we crossed transgenic individuals to Bristol and scored lethality among embryos from three crosses: self-fertilizing F_1 hermaphrodites, F_1 males backcrossed to Hawaii hermaphrodites, and Bristol × Hawaii F_1 males backcrossed to transgenic hermaphrodites. In the second cross, the transgene is inherited through the sperm, whereas in the third it is inherited through the oocyte. All crosses showed a reduction in embryonic lethality for transformants carrying fosmid B but not for those carrying fosmid A (Fig. 5). The ability of the transgene to mediate rescue when inherited through either sperm or oocyte implied that rescue occurs through zygotic transcription of *zeel-1*$_{Bristol}$. We genotyped surviving self-cross and male backcross progeny and found that survival of *zeel-1*$_{Hawaii}$ homozygotes required inheritance of the transgene, further supporting the idea that *zeel-1* acts zygotically (table S3).

To identify *zeel-1*, we individually subcloned the four predicted genes carried by fosmid B (Fig. 2A), introduced each into Hawaii, and tested for rescue. Only one subclone, containing predicted open reading frame *Y39G10AR.5*, rescued lethality, indicating that this gene is *zeel-1* (Fig. 5). *zeel-1* belongs to a previously uncharacterized *Caenorhabditis*-specific family of genes with homology to *zyg-11*, the substrate-recognition subunit of a CUL-2–based E3 ubiquitin ligase complex (17). *zeel-1* is located within the divergent interval and is deleted in Hawaii and all Hawaii-compatible wild isolates (table S2). To test whether

Table 2. Genes in the interval of elevated divergence between the Bristol and Hawaii haplotypes exhibit signatures of purifying selection. d_N, nonsynonymous substitutions per nonsynonymous site. d_S, synonymous substitutions per synonymous site. ω, the d_N/d_S ratio. These quantities were estimated by maximum likelihood with the PAML program (35).

Gene	No. of sites	d_N	d_S	ω
		To the left of the divergent interval		
Y39G10AR.7	1422	0.001	0.000	–
mcm-4	2469	0.000	0.004	–
Y39G10AR.15	2112	0.001	0.000	–
		Inside the divergent interval		
srbc-64	870	0.018	0.147	0.124
Y39G10AR.16*	681	0.019	0.106	0.181
ugt-31	1563	0.022	0.158	0.140
		On the right boundary of the divergent interval		
nekl-1†	2949	0.001	0.019	0.050

*The Hawaii and Bristol sequences have different predicted splice sites on both sides of intron 3, resulting in several predicted amino acid residues that are not shared between the two alleles. We considered only the shared exonic sequences. †*nekl-1* cDNAs from Bristol and Hawaii differ slightly from the predicted exon structure. We used the exon structure from our cDNA clones (8).

transgenic rescue requires ZEEL-1 protein, we generated a second *zeel-1* subclone identical to the first except that it contained a frame shift [via a 4–base pair (bp) insertion] truncating the protein at 25% of its length. When bombarded into Hawaii, the frameshifted transgene failed to rescue, indicating that rescue requires ZEEL-1 protein (Fig. 5).

Analysis of peel-1. Transgenic worms carrying Bristol-library fosmids, which together cover seven of the nine predicted genes in the *peel-1* interval, failed to induce the paternal-effect lethality of *zeel-1*$_{Hawaii}$ homozygotes, as did worms carrying subclones of the four genes within the divergent interval (8). Putatively null alleles of *srbc-64*, *nekl-1*, and *Y39G10AR.17*, as well as RNA interference (RNAi) targeting the remaining genes, did not abolish the paternal effect (tables S4 and S5). These negative results are equivocal because of potential germline silencing of transgenes, a possible requirement for chromosomal heterozygosity of *peel-1* in the spermatogenic germline, and the ineffectiveness of RNAi against sperm-expressed genes (18).

To find potential *peel-1* mutations, we examined the doubly compatible wild strain MY19 from Roxel, Germany. MY19 shows no lethality in crosses with Bristol and carries an intact *zeel-1* sequence, but it also fails to induce paternal-effect lethality in crosses with Hawaii, suggesting that it carries a Hawaii-like allele of *peel-1* or a suppressor of the paternal effect. To test for the existence of an unlinked suppressor, we mapped the inability of MY19 to induce lethality of *zeel-1*$_{Hawaii}$ homozygotes relative to a marker 10 cM from the *peel-1* interval (8). Absence of the paternal effect in MY19 mapped 10 cM from the marker (table S6), suggesting that MY19 might carry a mutation in *peel-1*. We sequenced all coding regions contained within the *peel-1* interval in MY19, as well as most noncoding regions located within the interval of elevated divergence between Bristol and Hawaii.

The MY19 haplotype is nearly identical to Bristol and contains only 12 nonsynonymous

polymorphisms, 4 of which fall in genes for which putative null alleles failed to abolish the paternal effect. Of the remaining polymorphisms, seven fall in *Y39G10AR.15*, a gene with spermatogenic germline expression (19) but located outside the divergent interval. The sequence of *Y39G10AR.16*, another gene with spermatogenic expression (19) but located within the divergent interval, contains no nonsynonymous polymorphisms. Notably, the coding sequence of *zeel-1*$_{MY19}$ is identical to that of *zeel-1*$_{Bristol}$, suggesting that the paternal effect does not arise from the activity of *zeel-1* itself or that if it does, MY19 and Bristol differ in their regulatory regions.

Discussion. We discovered a genetic incompatibility in *C. elegans* that causes lethality of embryos homozygous for a naturally occurring deletion of *zeel-1* when sired by individuals heterozygous for the Bristol and Hawaii alleles of a tightly linked paternal-effect gene, *peel-1*.

Paternal-effect mutations are rare, and only one has been described in *C. elegans* (20). The interaction between a paternal effect and a zygotically acting gene is surprising given that sperm-supplied factors are expected to act before zygotic transcription begins (9, 10). Zygotically expressed ZEEL-1 may be a molecular antidote to a sperm-carried PEEL-1 protein that is otherwise toxic during development. An analogous maternal effect by zygotic interaction has been described in *Tribolium* (21).

The Bristol haplotype of the *zeel-1/peel-1* interval gains a transmission advantage by inducing the lethality of embryos not inheriting it. This segregation distortion is characteristic of genic drive, in which selection at the level of alleles within an individual (genic selection) acts independently of selection at the level of individuals within a population (genotypic selection). Aside from this similarity, however, the *C. elegans* incompatibility does not conform to the expectations of genic drive. In drive systems, driver haplotypes are expected to fix within populations and are observed only where
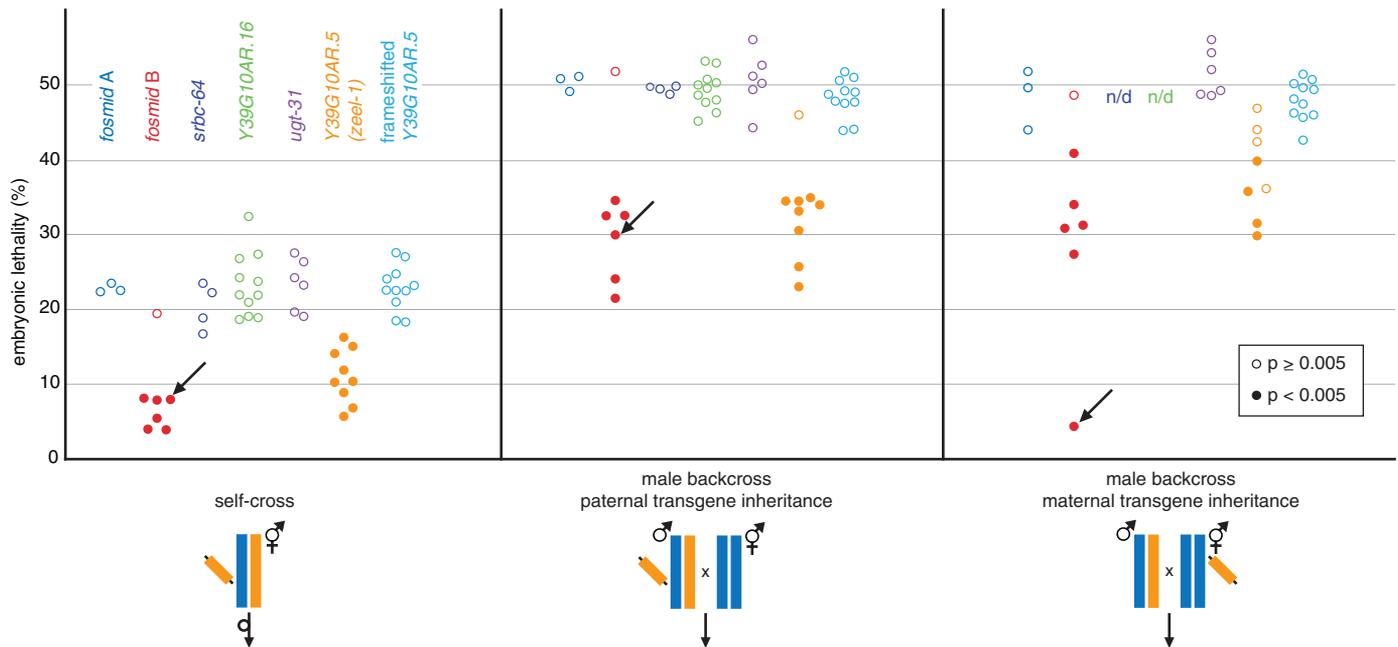
Fig. 5. Transgenic complementation identifies *Y39G10AR.5* as *zeel-1*. Embryonic lethality was scored in three crosses: selfing F₁ hermaphrodites carrying the transgene, Hawaii hermaphrodites × F₁ males carrying the transgene, and Hawaii hermaphrodites carrying the transgene × F₁ males. Orange and blue bars designate Bristol and Hawaii haplotypes, respectively. Diagonal segments represent transgenes. Within crosses, each circle represents the result for an independent transgenic line (n/d, not determined). For each result, we scored at least 50 embryos; typically, 200 to 300 were scored. Solid circles mark results showing a significant reduction in lethality (one-sided χ^2, $P < 0.005$). Most transgenes were not integrated and were therefore not transmitted to all progeny. Arrows designate the single integrated line. In the male backcross with maternal transgene inheritance, where the integrated transgene was transmitted to all progeny, embryonic lethality was 4% ($n = 298$ embryos).

genotypic selection against them prevents fixation (*22*). Where this countervailing force is absent, drivers become fixed in a population and are detectable only in interpopulation crosses (*23–27*). In *C. elegans*, homozygotes of both haplotypes are fit, and incompatible haplotypes co-occur globally. One explanation for the long-term maintenance of both haplotypes is that genotypic selection favoring the Hawaii haplotype counterbalances genic drive favoring Bristol. Because *C. elegans* is primarily selfing and drive can influence transmission only in heterozygotes, this model would require a precise and stable level of outcrossing. Although a lack of knowledge of *C. elegans* population biology prevents us from rejecting this model, we favor an alternative explanation not subject to such constraints.

Whereas the drive model implies that balancing selection is a consequence of the incompatibility, an alternative is that the incompatibility is an incidental side effect of balancing selection. For example, balancing selection on pathogen resistance genes with costs in the absence of infection may maintain two haplotypes within a population for much longer than would be possible under neutral drift (*28, 29*). If the haplotypes occur largely as homozygotes within a primarily selfing species, mutations arising on one haplotype are rarely tested against mutations on the other. Alleles fixed by drift or positive selection within the genetic context of their own haplotype but incompatible with alleles of another are not purged from the population but instead maintained alongside the balanced polymorphism, which acts as an incompatibility trap. Because incompatible alleles are deleterious only after outcrossing, selection favoring the balanced polymorphism may be of lesser magnitude than selection against the incompatibility. Because long-term maintenance of incompatible alleles depends on tight linkage to the balanced polymorphism, the interacting loci are necessarily tightly linked to one another as well.

Our model, like genic drive, explains the occurrence of long-lived incompatible alleles at tightly linked loci, but it better incorporates the low level of outcrossing and the global co-occurrence of both haplotypes. Although the cause of balancing selection remains unknown, all genes within the divergent interval carry multiple nonsynonymous differences between the haplotypes, and several are known or predicted to interact with signals from the environment (*30–32*). The deletion of *zeel-1* may be analogous to presence/absence polymorphisms of pathogen resistance genes in *Arabidopsis*, which are known targets of balancing selection (*28, 29*).

The *C. elegans* incompatibility suggests that long-term balancing selection in selfing species may facilitate the sympatric accumulation and maintenance of Dobzhansky-Muller type incompatibilities involving tightly linked loci. In the Dobzhansky-Muller model of speciation, incompatibilities emerge from the deleterious interactions of alleles that are neutral or advantageous in their own genetic backgrounds. Although classic models predict incompatible alleles to occur in allopatric populations (*33*), the *C. elegans* incom-patibility occurs within interbreeding populations and does not appear to precipitate speciation, because gene flow between the incompatible classes occurs throughout the rest of the genome. The *C. elegans* incompatibility may be an example of incidental linkage between developmentally and ecologically important genes driving the evolution of development.

References and Notes
1. A. Barrière, M. A. Félix, *Curr. Biol.* **15**, 1176 (2005).
2. J. Hodgkin, T. Doniach, *Genetics* **146**, 149 (1997).
3. A. Barrière, M. A. Félix, *Genetics* **176**, 999 (2007).
4. A. Sivasundar, J. Hey, *Curr. Biol.* **15**, 1598 (2005).
5. D. R. Denver, K. Morris, W. K. Thomas, *Mol. Biol. Evol.* **20**, 393 (2003).
6. K. A. Swan *et al.*, *Genome Res.* **12**, 1100 (2002).
7. S. R. Wicks, R. T. Yeh, W. R. Gish, R. H. Waterston, R. H. Plasterk, *Nat. Genet.* **28**, 160 (2001).
8. See supporting material on *Science* Online.
9. S. W. L'Hernault, "Spermatogenesis" (20 February 2006), at WormBook, The *C. elegans* Research Community, doi/10.1895/wormbook.1.85.1 (www.wormbook.org).
10. P. Gonczy, L. S. Rose, "Asymmetric cell division and axis formation in the embryo" (15 October 2005), at WormBook, The *C. elegans* Research Community, doi/10.1895/wormbook.1.30.1 (www.wormbook.org).
11. M. Haber *et al.*, *Mol. Biol. Evol.* **22**, 160 (2005).
12. R. Koch, H. G. van Luenen, M. van der Horst, K. L. Thijssen, R. H. Plasterk, *Genome Res.* **10**, 1690 (2000).
13. A. Sivasundar, J. Hey, *Genetics* **163**, 147 (2003).
14. D. Charlesworth, *PLoS Genet.* **2**, e64 (2006).
15. A. D. Cutter, *Genetics* **172**, 171 (2006).
16. D. R. Denver, K. Morris, M. Lynch, W. K. Thomas, *Nature* **430**, 679 (2004).
17. S. Vasudevan, N. G. Starostina, E. T. Kipreos, *EMBO Rep.* **8**, 279 (2007).
18. J. Ahringer, "Reverse genetics" (6 April 2006), at WormBook, The *C. elegans* Research Community, doi/10.1895/wormbook.1.47.1 (www.wormbook.org).

19. V. Reinke, I. S. Gil, S. Ward, K. Kazmer, *Development*
    131, 311 (2004).
20. H. Browning, S. Strome, *Development* **122**, 391
    (1996).
21. R. W. Beeman, K. S. Friesen, R. E. Denell, *Science* **256**,
    89 (1992).
22. G. D. Hurst, J. H. Werren, *Nat. Rev. Genet.* **2**, 597
    (2001).
23. A. Atlan, H. Mercot, C. Landre, C. Montchamp-Moreau,
    Evol. Int. J. Org. Evol. **51**, 1886 (1997).
24. R. W. Beeman, K. S. Friesen, *Heredity* **82**, 529 (1999).
25. L. Fishman, J. H. Willis, *Genetics* **169**, 347 (2005).
26. H. A. Orr, S. Irving, *Genetics* **169**, 671 (2005).
27. F. A. Reed, R. G. Reeves, C. F. Aquadro, *Evol. Int. J. Org.
    Evol.* **59**, 1280 (2005).
28. E. A. Stahl, G. Dwyer, R. Mauricio, M. Kreitman,
    J. Bergelson, *Nature* **400**, 667 (1999).
29. D. Tian, H. Araki, E. Stahl, J. Bergelson, M. Kreitman,
    Proc. Natl. Acad. Sci. U.S.A. **99**, 11525 (2002).
30. M. Shapira *et al.*, *Proc. Natl. Acad. Sci. U.S.A.* **103**,
    14086 (2006).
31. J. H. Thomas, *Genome Res.* **16**, 1017 (2006).
32. J. H. Thomas, *Genetics* **172**, 127 (2006).
33. H. A. Orr, D. C. Presgraves, *Bioessays* **22**, 1085 (2000).
34. K. A. Frazer, L. Pachter, A. Poliakov, E. M. Rubin,
    I. Dubchak, *Nucleic Acids Res.* **32**, W273 (2004).
35. Z. Yang, *Comput. Appl. Biosci.* **13**, 555 (1997).
36. We thank the *Caenorhabditis* Genetics Center, the National
    Bioresource Project of Japan, the NemaGENETAG Consortium,
    M.-A. Félix, A. Barrière, E. Dolgin, and H. Van Epps for strains;
    R. Maruyama and A. Singson for advice; S. Skrovanek for
    lab assistance; and H. Coller, A. Cutter, D. Gresham, R. Gosh,
    L. Moyle, J. Shapiro, and E. Smith for comments on the
    manuscript. Supported by a National Defense Science and

REPORTS

Single-Molecule Cut-and-Paste Surface Assembly

S. K. Kufer,[1] E. M. Puchner,[1] H. Gumpp,[1] T. Liedl,[2] H. E. Gaub[1]

We introduce a method for the bottom-up assembly of biomolecular structures that combines the precision of the atomic force microscope (AFM) with the selectivity of DNA hybridization. Functional units coupled to DNA oligomers were picked up from a depot area by means of a complementary DNA strand bound to an AFM tip. These units were transferred to and deposited on a target area to create basic geometrical structures, assembled from units with different functions. Each of these cut-and-paste events was characterized by single-molecule force spectroscopy and single-molecule fluorescence microscopy. Transport and deposition of more than 5000 units were achieved, with less than 10% loss in transfer efficiency.

Functional biomolecular assembly aims to create structures from a large variety of biomolecular building blocks in a geometrically well-defined manner in order to create new functions (*1*, *2*), such as artificial signaling cascades or synergetic combinations of enzymes. Hybrid devices could include quantum dots co-assembled with dye molecules, or gold particles assembled as plasmon hot spots with a sample protein positioned into the focus (*3*). One way to assemble such molecular devices would be to physically pick up the different units needed with a scanning probe tip, translocate these units to a different location, and deposit them with high spatial precision (*4–6*). The entire process would also have to be carried out in an aqueous environment.

For the translocation of nanoscale objects, we used atomic force microscopy, which has been used in this context for mechanical single-molecule experiments (*7–12*) or lithography (*13*, *14*); however, previously suggested devices include the use of molecular pliers at the end of atomic force microscope (AFM) cantilevers that could grab and release the building blocks, triggered by an external signal of either electrical or optical nature (*15*). We report a simpler and robust solution based on DNA hybridization and hierarchical bonds defined by different unbinding forces.

A well-sorted "depot," with a large variety of molecular species, stably stored in well-defined loci, is a prerequisite for the assembly of a multi-component device. DNA chips offer a freely programmable pattern of oligomers that are commercially available and have spot sizes in the submicrometer range (*16*). Niemeyer *et al.* (*17*) converted such a DNA pattern into a protein pattern by binding a DNA-labeled protein to its corresponding spot on a DNA chip. The length of the oligomers can be chosen so that after incubation and stringent washing, a thermodynamically stable pattern of proteins is obtained. Given the known sequence map of the DNA chip, different molecular species can be stored in a known position on the depot chip. Alternatively, when only a limited variety of building blocks is needed, microfluidic elastomer channels may be used to create patterns (*18–20*) of building blocks, which after removal of the elastomer may be manipulated with the AFM tip (fig. S3).

We used this approach to store our functional units and also extended the DNA oligomers to fulfill a second function; namely, to serve as a handle (Fig. 1). This additional stretch of DNA can hybridize to a complementary DNA covalently attached to an AFM tip. We chose the duplexes to be comparable in length and binding free energy, but we selected the sequences so that the anchor hybridizes in the so-called "unzip" geometry and the handle hybridizes in the "shear" geometry [Fig. 1 and (*21*)]. These two duplex geometries differ substantially in that, upon forced unbinding, the zipper duplex is opened up base pair by base pair, whereas in the shear geometry, all base pairs are loaded in parallel (Fig. 2 and fig. S1). Although the thermodynamic stability and the spontaneous off rate of both geometries are comparable, their rupture forces differ dramatically (*22*), as has been shown experimentally and was validated theoretically in several studies (*21*, *23–27*). Thus, upon retraction of the AFM tip, the anchor duplex will break open and the functional unit will be bound to the tip.

As can be seen in Fig. 2C, these force distance curves provide a characteristic fingerprint and serve as a robust criterion to decide whether a molecule was picked up from the depot. To avoid multiple transfers, we chose the density of the anchors on the tip to be low enough that in 35% of the attempts, only one unit was picked up, and in 20% of the attempts, just two units. In 20% of all attempts, we recorded traces like the lower two in Fig. 2C, which showed that we had not picked up any unit (fig. S5D). Because we recorded such a force distance curve for every pickup, we knew exactly how many units were transferred to the tip. The pickup process can be corrected online by either picking up more units or by dropping excess units in a "trash can" on the target area.

Once a unit is transferred to the tip, it can be moved to its new position on the target area. The target area had surface chemistry similar to that of the depot area, but the anchor oligomers were chosen so that when the tip was lowered, they bound to the transfer DNA in shear geometry and formed a duplex, which was longer than the handle duplex. Although the AFM tip can be positioned with subnanometer reproducibility, the precision with which the units can be

[1]Center for Nanoscience and Department of Physics, University of Munich, Amalienstrasse 54, 80799 Munich, Germany. [2]Department of Biological Chemistry and Molecular Pharmacology, Harvard Medical School, and Department of Cancer Biology, Dana-Farber Cancer Institute, Boston, MA 02115, USA.